

PACS numbers: 31.15.es, 61.46.Bc, 71.20.-b, 73.22.-f, 81.05.Zx, 81.07.Pr, 82.35.Np

Design and Exploring the Structure and Electronic Characteristics of PS/MnO₂/NiO Nanosystem for Optics and Electronics Nanodevices

Ali S. Hasan¹, Ahmed Hashim², and Zinah S. Hasan³

¹*College of Materials Engineering,
Department of Polymer and Petrochemical Industries,
University of Babylon,
Hillah, Iraq*

²*College of Education for Pure Sciences,
Department of Physics,
University of Babylon,
Hillah, Iraq*

³*Babylon Technical Institute,
Al-Furat Al-Awsat Technical University,
Najaf, Iraq*

The present work comprises design of new polystyrene (PS)/MnO₂/NiO nanosystem to exploit it in many optics and electronics nanodevices. The optimization, structural and electronic characteristics of PS/MnO₂/NiO nanosystem are studied. The results indicate that the electronics characteristics of PS are improved, when the MnO₂/NiO nanostructures are added. The energy gap of PS is decreased from 5.773 eV to 3.814 eV with adding of MnO₂/NiO nanostructures. The results show that the PS/MnO₂/NiO nanosystem has excellent electronic characteristics, which make the PS/MnO₂/NiO nanosystem suitable for different optics and electronics fields.

Ця робота включає проєктування нової наносистеми полістирол (ПС)/MnO₂/NiO для використання в багатьох оптичних і електронних нанопристроях. Досліджено оптимізацію, структуру й електронні характеристики наносистеми ПС/MnO₂/NiO. Результати показали, що електронні характеристики полістиролу було поліпшено із додаванням наноструктур MnO₂/NiO. Енергетична заборонена зона ПС зменшилася від 5,773 еВ до 3,814 еВ через додавання наноструктур MnO₂/NiO. Остаточні результати показали, що наносистема ПС/MnO₂/NiO має відмінні електронні характеристики, які роблять наносистему ПС/MnO₂/NiO придатною для різних областей оптики й електроніки.

Key words: polystyrene, MnO₂/NiO, nanosystem, electronic characteris-

tics, energy gap.

Ключові слова: полістирол, MnO_2/NiO , наносистема, електронні характеристики, енергетична заборонена зона.

(Received 3 September, 2023)

1. INTRODUCTION

Composite materials have a wide variety of applications in electrical devices, mobile communication systems, *etc.* Therefore, composite tailoring was initiated to suit the specific needs for different usage. In the past decade, there have been several researches carried out with different metal oxides due to their application in various electronic devices such as smart window, optical detector, cathode coating in high-capacity lithium batteries, high performance capacitor, thermistor and others. Transition elements have mixed valence ions; hence, those compounds have unique properties and are very useful in various fields [1]. Nanostructured manganese dioxide (MnO_2) is a promising transition metal oxide for its admirable chemical stability, transparency, low toxicity, low cost, functional biocompatibility, excellent adsorption capacity, catalytic properties, and widespread availability [2].

Nickel oxide (NiO) is the most investigated metal oxide and it has attracted considerable attention because of its low cost material, and also for its application in several fields such as a catalyst, transparent conducting oxide, photodetectors, electrochromic, gas sensors, photovoltaic devices, electrochemical supercapacitors, heat reflectors, photoelectrochemical cell, solar cells and many optoelectronic devices. NiO is an IV group and it can be used as a transparent *p*-type semiconductor layers, it has a band gap energy ranging from 3.45 eV to 3.85 eV. Band gap energy is significant to adjust the energy level state of NiO [3]. Polystyrene (PS) is a commercial thermoplastic polymer. It is rather brittle, clear and has good mechanical properties and a low cost price. Thus, PS has a wide range of applications as construction materials, packaging, disposable cups, consumer electronics, cassette boxes, compact disks and medical uses [4]. There are several studies on the electronic, optical and electrical properties of polystyrene nanocomposites [5–11]. The current study includes design of $\text{PS}/\text{MnO}_2/\text{NiO}$ nanostructures and investigating the electronic properties to employ in various optoelectronics nanodevices.

2. COMPUTATIONAL DETAIL

In this work, all the geometric structures are optimized and considered by time-dependent density-functional theory (TDDFT) with

B3LYP [12, 13] functional and the 6-31G (d , p) basis set, which applied in Gaussian 09 software [14]. TDDFT methods provide a powerful approach for studying the electronic structure and properties of molecules. They offer several advantages that contribute to enhancing the accuracy and reliability of computational results in comparison to other methods. TDDFT allows for the investigation of excited electronic states, which are crucial for understanding phenomena such as absorption spectra, fluorescence, and photochemical reactions. By including the description of excited states, TDDFT can provide a more comprehensive understanding of molecular behaviour. In addition, TDDFT is computationally more efficient compared to methods based on wave function theory, such as traditional *ab initio* methods. TDDFT calculations scale linearly with system size, making it feasible to study larger systems and perform more extensive sampling of potential energy surfaces. One of the most important reasons for choosing a method TDDFT is applicable to a wide range of molecular systems, including organic molecules, inorganic complexes, and materials, especially polymers. It can be used to investigate various properties, such as electronic spectra, response properties, and excited-state dynamics. This chemical model has been extensively used to relax the geometry and calculate the optoelectronic properties, such as total energies (E_T), Fermi energy (E_F), HOMO (Highest Occupied Molecular Orbital) and LUMO (Lowest Unoccupied Molecular Orbital), energy gap (E_g) and electronic transition energies. These methods are not only encouraging more profound understanding of the association between the optoelectronic properties and chemical structures of the molecule structures but also may be used to design new molecule structures. To evaluate the reactivity and the stability of the composites, TDDFT-based descriptors were calculated [15, 16]:

$$\mu = \left(\frac{\partial E}{\partial N} \right)_{V(\mathbf{r}), T}, \quad \eta = \frac{1}{2} \left(\frac{\partial^2 E}{\partial N^2} \right)_{V(\mathbf{r}), T}, \quad S = \frac{1}{2\eta}, \quad \omega = \frac{\mu^2}{2\eta},$$

where I_p , E_A , μ , η , S , and ω are the ionization potential, electron affinity, chemical potential, chemical hardness, chemical softness, and electrophilicity, respectively, while E , N and $V(\mathbf{r})$ are the total electron energy, number of electrons, and external potential, respectively. There are two different methods to calculate the above the global quantities, the first is a finite difference approximation which based on the differences of total electronic energies when an electron is removed or added in accordance with the neutral molecule [17]. The second is Koopmans' theorem, which based on the differences between the HOMO and LUMO energies for the neutral molecule [13]. Using a finite difference approximation, the global

quantities can be given by [18–20] as follow:

$$I_P = -E_{HOMO}, E_A = -E_{LUMO}, \eta = \frac{(I_P - E_A)}{2}.$$

Then, using Koopmans' theorem, the above equations can be given as follow:

$$E_F = \frac{(E_{HOMO} + E_{LUMO})}{2}, \eta = \frac{(E_{HOMO} - E_{LUMO})}{2}.$$

3. RESULTS AND DISCUSSION

In this research study, computational analyses were conducted using the Gaussian 09 suite of programs and the TDDFT methods to investigate certain molecules, as shown in Fig. 1. The focus was on the geometrical optimization of polystyrene (PS) and PS-MnO₂-NiO structures. The relaxation process aimed to find the most stable configurations for these structures based on the computational analyses. In the research study, computational analyses were conducted using Gaussian 09, a widely recognized software package for computational chemistry [17, 21, 22]. To improve the accuracy and reliability of the results, the study employed Time-Dependent Density Functional Theory (TDDFT) methods.

Specifically, the carbon-carbon bond lengths fell within the ranges for C–C: 1.511 Å, C=C: 1.401 Å, and C–H: 1.057 Å. Additionally, the bond lengths for Mn–O and Ni–O were determined to be 1.83 Å and 1.748 Å, respectively. These values are consistent with the typical bond lengths observed in aromatic rings [18, 23, 24]. The

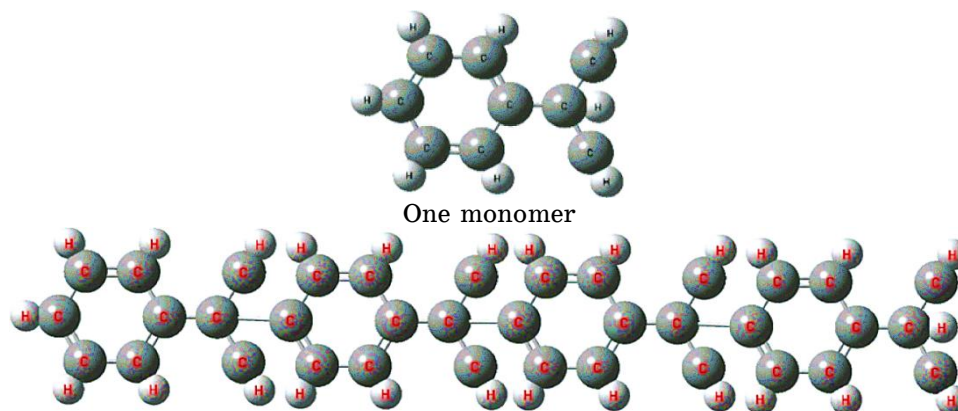


Fig. 1. Structural of PS before relaxing.

bond length between carbon and hydrogen in organic molecules can be influenced by electrostatic forces between molecules, influenced by positive or negative charges, can influence electron transfer and impact the bond length. In addition, hydrogen bonding interactions and other intermolecular forces can also influence the bond length between carbon and hydrogen. Hydrogen bonding can lead to elongation or contraction of the bond length, depending on the strength and directionality of the hydrogen bond. As well, molecules can go through transition states where bond lengths may deviate from their equilibrium values. Factors such as reaction pathways, activation energies, and intermediate states can temporarily affect the bond length between carbon and hydrogen [24–26].

The research focused on the geometrical optimization of polymeric composites, specifically PS and PS-MnO₂-NiO. The obtained structural properties were found to be in good agreement with experimental data, both in terms of bond length and bond strength. This agreement suggests that these materials exhibit interactions and properties that are highly compatible with each other from both physical and chemical perspectives, as illustrated in Figs. 2 and 3.

The compatibility observed between PS and the MnO₂-NiO composite implies that they can effectively interact with each other,

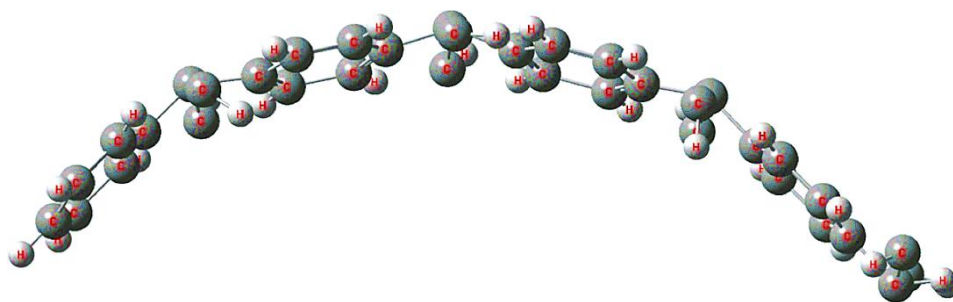


Fig. 2. Structure of PS after relaxing.

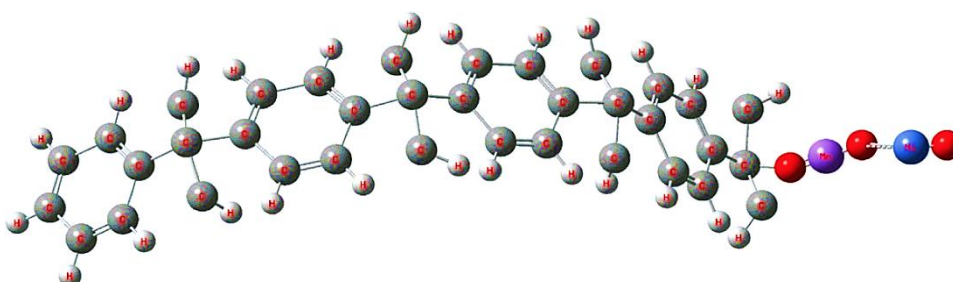


Fig. 3. Structure of PS-MnO₂-NiO composites.

leading to the formation of new compounds or compounds in a consistent and homogeneous manner. The presence of MnO_2 and NiO in the composite can create a favourable environment for chemical reactions with PS. These metal oxides can act as catalysts or initiators, facilitating chemical reactions with the polymer. This compatibility opens up possibilities for joint applications or the creation of composite compositions that can benefit from the combined interactions of these materials.

With the observation of Fig. 3 after relaxation, we notice the significant change in the shape of the polymer chain, so that PS and the MnO_2 - NiO compound participate in intermolecular interactions, such as hydrogen bonding, van der Waals forces, or stacking interactions. Thus, these interactions promote the alignment and aggregation of the polymer chains with the composite, leading to the formation of new structures or phases within the composite material [17, 27].

Table presents the ground state calculations of polymeric composites in this study, specifically focusing on the minimum energy configurations. The calculations include the following parameters: total energy (in atomic units, [a.u.]), I_p and E_A (measured in [eV]) calculated using Koopmans' theorem, E_g in [eV], S in $[(\text{eV})^{-1}]$, η in [eV], ω in [eV], density of states (DOS) and the energies of the HOMO and LUMO. E_T of the polymeric composites in this study is observed to be very small. This indicates that the binding energy within each structure is also low. Consequently, polymeric composites with lower total energy tend to have limited energy storage capabilities. However, this characteristic can be advantageous in certain applications that prioritize lightweight materials. The specific selection or composition of the composites plays a crucial role in achieving these properties [18, 22, 27].

Where lightweight materials play a crucial role in renewable energy technologies? For instance, in wind energy, lightweight composite materials are used for turbine blades to enable efficient energy conversion. Similarly, in solar energy, lightweight materials are utilized for constructing solar panels and supporting structures. In addition, lightweight materials are integral to portable electronic devices such as smartphones, laptops, and tablets. Materials like aluminium, magnesium alloys, and polymers are used to reduce weight and enhance portability without compromising durability [18, 19, 28].

Indeed, the I_p and E_A values can vary between different materials or composite systems. In the case of PS- MnO_2 - NiO , both the I_p and E_A values are higher compared to PS. A higher I_p indicates that the material has a stronger tendency to retain its electrons, while a higher E_A suggests a greater ability to attract additional electrons.

TABLE. Calculation total energies (E_T), HOMO energies (E_{HOMO}), LUMO energies (E_{LUMO}), electronic band gap (E_g), Fermi energies (E_F), ionization potentials (I_p), electron affinities (E_A), chemical potentials (μ), chemical hardnesses (η), chemical softnesses (S) and electrophilicity indexes (ω) (in [eV]) *via* using TDDFT B3LYP/6-31 (d , p) scheme.

Sample	E_T	HOMO	LUMO	E_g	I_p	E_A	E_F	η	S	ω
PS	-9541.325	-5.9874	-0.2147	5.773	5.987	0.215	-3.101	2.886	0.173	1.666
PS-MnO ₂ -NiO	-6378.325	-4.0124	-0.1987	3.814	4.012	0.199	-2.106	1.907	0.262	1.163

These differences in electronic properties between composites can be attributed to several factors, including variations in chemical composition, structure, or bonding characteristics, where the incorporation of MnO_2 and NiO into the PS matrix can introduce additional electron-donating or electron-accepting groups, altering the overall electronic behaviour of the composite. Changes in the composite's chemical environment, such as the presence of transition metal ions or different bonding configurations, can also influence the I_p and E_A values. Understanding these electronic property differences is crucial for tailoring the behaviour and functionality of polymeric composites for specific applications, such as energy storage, catalysis, or electronic devices [14, 16, 29].

The results obtained for the parameters S , η , and ω in the structures PS and PS- MnO_2 - NiO indicate important characteristics of the polymeric composites. A large value of η and ω suggests a higher energy requirement, indicating that the system is relatively more stable and less reactive towards electron transfer, whereas shown in Table. This one indicates that the polymeric composites have a greater energy threshold for electron transfer processes, making them less prone to electronic changes or reactivity. On the other hand, a small value of S suggests a lower energy requirement for electron transfer, implying higher reactivity and a greater tendency to undergo electronic changes. This can be attributed to the compatibility and good distribution of materials within the polymer matrix, which facilitates electron transfer processes and enhances reactivity [19]. Additionally, it is observed that the chemical hardness decreases and the chemical softness increases in both PS and PS- MnO_2 - NiO structures. Higher values of chemical softness indicate a lower energy requirement for electron transfer, implying greater reactivity and a higher propensity for electronic changes. The compatibility and good distribution of the materials within the polymer matrix contribute to these changes in chemical hardness, softness, and electrophilicity. The specific arrangement and distribution of the MnO_2 and NiO components within the polymer matrix enhance the reactivity and electronic changes in the composite [30, 31].

The concepts of chemical hardness, softness, and electrophilicity are relevant in understanding the reactivity and stability of polymeric composites. A decrease in chemical hardness and an increase in chemical softness indicate a lower energy requirement for electron transfer, implying higher reactivity and a greater tendency to undergo electronic changes. This is attributed to the compatibility and good distribution of materials within the polymer matrix. Changes in these properties can have implications for the design and application of polymeric composites in areas such as catalysis, energy storage, and electronic devices [14].

Through the Table, the information suggests that the addition of $\text{MnO}_2\text{-NiO}$ to the polymer PS leads to a decrease in the E_g values, indicating a decrease in the energy gap between the HOMO and LUMO levels. This suggests the possibility of an electronic transition between the valence band and conductivity. When $\text{MnO}_2\text{-NiO}$ is added to the polymer, it interacts with the existing polymer structures through various mechanisms, such as chemical bonding, electrostatic interactions, and intermolecular forces. These interactions can result in changes in the electronic structure of the polymer and the formation of new energy states within the polymer. One possible mechanism is the formation of chemical bonds between the $\text{MnO}_2\text{-NiO}$ particles and the polymer chains. This can occur through covalent bonding or coordination bonding, depending on the nature of the materials and the specific conditions. The formation of chemical bonds introduces new energy levels within the polymer electronic structure. Additionally, the presence of $\text{MnO}_2\text{-NiO}$ particles can induce changes in the local electric field and electronic environment around the polymer chains. This can lead to polarization effects and redistribution of electron density within the polymer. As a result, new energy states may emerge within the polymer's electronic band structure [15, 21, 31].

Figures 4 and 5 depict the HOMO and LUMO energy levels for

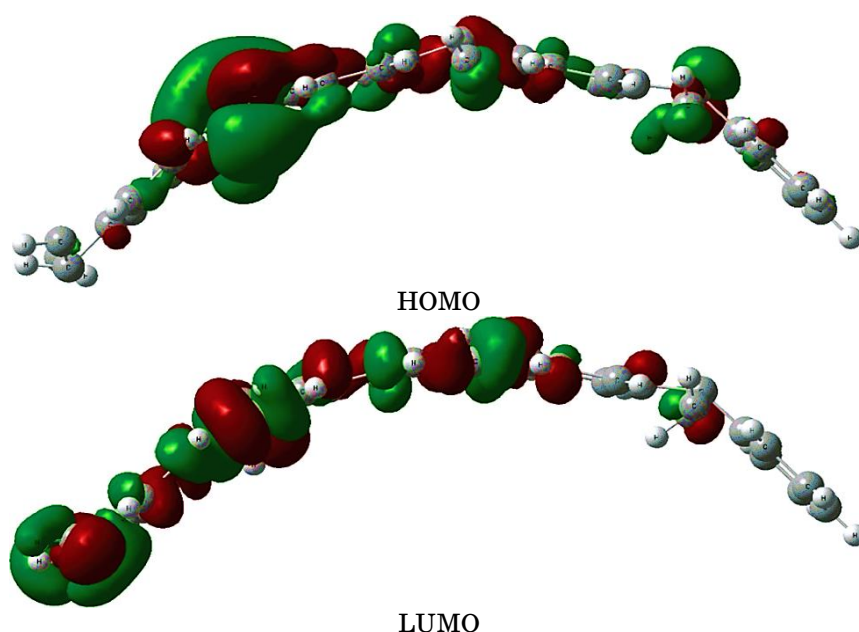


Fig. 4. The shapes of HOMO and LUMO for PS.

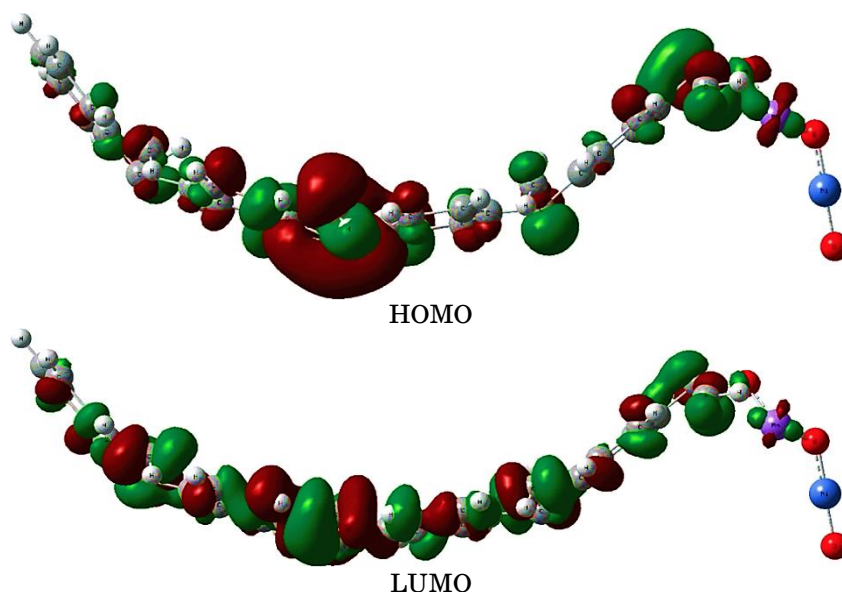


Fig. 5. The shapes of HOMO and LUMO for PS-MnO₂-NiO composites.

the PS-MnO₂-NiO structure, showing a more stable electronic distribution compared to PS alone. This stability is likely due to the withdrawal of electrons by the MnO₂-NiO materials. This enhanced stability can be attributed to the withdrawal of electrons by the MnO₂-NiO materials. MnO₂-NiO, being transition metal oxide materials, can have a higher electron affinity compared to the polymer PS. This means that they have a stronger tendency to attract and accept electrons. When MnO₂-NiO is incorporated into the PS matrix, it can act as an electron acceptor, causing a redistribution of electron density within the system. As MnO₂-NiO withdraws electrons from the surrounding PS molecules, it can induce a more balanced distribution of electron density throughout the structure. This redistribution of electrons helps stabilize the electronic system by reducing any localized charge imbalances or electron-rich regions within the polymer [14, 29, 30].

The provided information highlights the significance of the density of states (DOS) in understanding the electronic structure and properties of materials. The DOS provides valuable insights into various material properties, including electrical conductivity, thermal conductivity, and optical properties. The DOS is a function of energy, denoted as $g(E)$, where E represents the energy level. It describes the number of states per unit volume per unit energy range at a specific energy level. Mathematically, the DOS can be expressed as follows:

$$g(E) = V^{-1}dN(E)/dE,$$

where V represents the volume of the material, and $dN(E)/dE$ represents the change in the number of states with respect to energy.

In the context of polymeric compounds, the density diagram or DOS plot (as shown in Figs. 6 and 7) reveals the presence of an en-

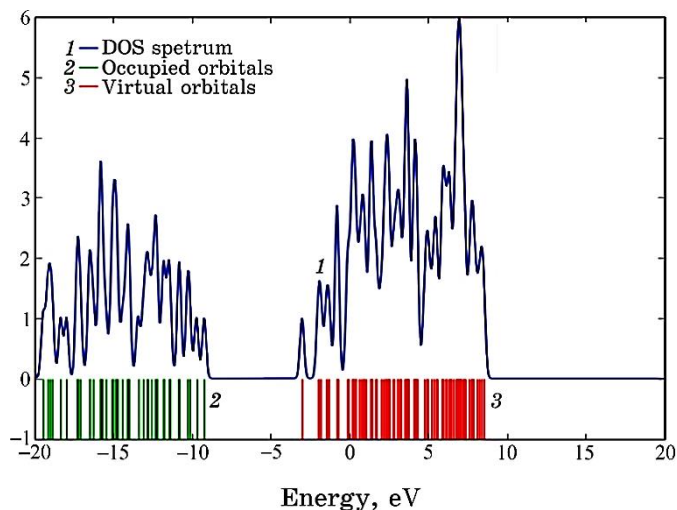


Fig. 6. Density of states (DOS) for PS.

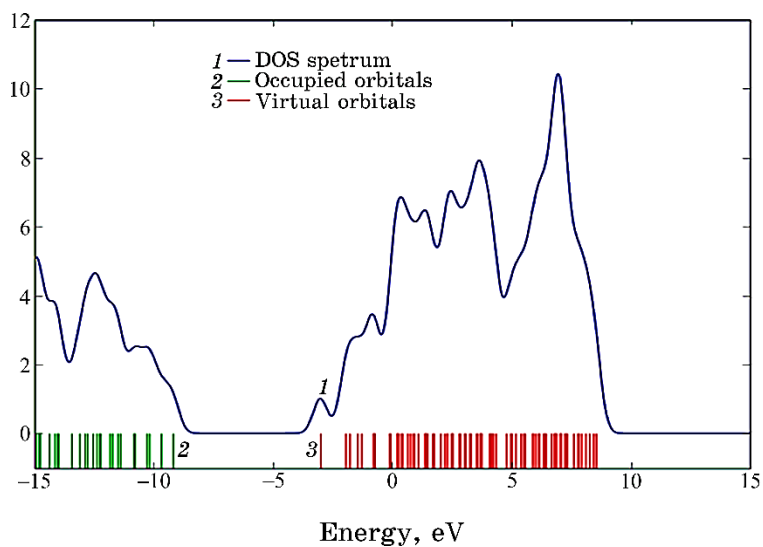


Fig. 7. Density of states (DOS) for PS-MnO₂-NiO composites.

ergy gap between the valence band (the highest occupied energy band) and the conduction band (the lowest unoccupied energy band) [17, 28].

Within the band gap, the DOS exhibits a region of either zero or very low density of states. This indicates a lack of available electronic states in that energy range. On the other hand, the DOS is relatively high in the valence and conduction bands, indicating the presence of occupied or excited electronic states. The presence of a distinct energy gap between the valence and conduction bands is a characteristic feature of semiconductors and insulators as in polymers. By analysing the DOS, researchers can study phenomena such as energy bands, and the E_F energy, which is a key concept in solid-state physics and is related to DOS. It represents the highest energy level that electrons occupy at a temperature of absolute zero. Moreover, as shown in Table, while the E_F increases when $\text{MnO}_2\text{-NiO}$ is added, this confirms that the E_F exists within the band gap in the polymers, which is the energy band where no electronic states are allowed. The DOS near the E_F in this region is low, reflecting the lack of available occupancy electronic states. This energy gap prevents large electron mobility and leads to poor electrical conductivity. However, in $\text{PS-MnO}_2\text{-NiO}$ composites, the band gap is relatively small compared to insulators, which allows some thermal excitation of electrons across the gap, leading to their partial conduction [25, 31].

4. CONCLUSIONS

This work involved design and investigating the optimization, structure and electronic characteristics of $\text{PS/MnO}_2\text{/NiO}$ nanosystem as a new nanostructure to utilize in a lot of optics and electronics applications. The obtained results illustrated that the electronics characteristics of polystyrene were improved, when the $\text{MnO}_2\text{/NiO}$ nanostructures added. The energy gap of PS decreased from 5.773 eV to 3.814 eV among adding of $\text{MnO}_2\text{/NiO}$ nanostructures. The final results indicated to the $\text{PS/MnO}_2\text{/NiO}$ nanosystem have excellent electronic characteristics, which make the $\text{PS/MnO}_2\text{/NiO}$ nanosystem appropriate for different optics and electronics applications.

REFERENCES

1. T. F. Khoon, J. Hassan, Z. A. Wahab, and R. S. Azis, *Results in Physics*, **6**: 420 (2016); <https://doi.org/10.1016/j.rinp.2016.07.011>
2. M. Zahan and J. Podder, *SN Applied Sciences*, **2**: 1 (2020); <https://doi.org/10.1007/s42452-020-2191-8>

3. M. Ghougali, O. Belahssen, and A. Chala, *Journal of Nano- and Electronic Physics*, **8**, No. 2: 1 (2016); doi:10.21272/jnep.8(4(2)).04059
4. G. M. Nasr, T. A. Mohamed, and R. M. Ahmed, *IOP Conf. Series: Materials Science and Engineering*, **956**: 1 (2020); doi:10.1088/1757-899X/956/1/012002
5. H. Ahmed and A. Hashim, *Silicon*, **15**: 2339 (2023); <https://doi.org/10.1007/s12633-022-02173-w>
6. H. Ahmed and A. Hashim, *Opt. Quant. Electron.*, **55**: 1 (2023); <https://doi.org/10.1007/s11082-022-04273-8>
7. M. H. Meteab, A. Hashim, and B. H. Rabee, *Silicon*, **15**: 1609 (2023); <https://doi.org/10.1007/s12633-022-02114-7>
8. A. Hashim, M. H. Abbas, N. A.-H. Al-Aaraji, and A. Hadi, *J. Inorg. Organomet. Polym.*, **33**: 1 (2023); <https://doi.org/10.1007/s10904-022-02485-9>
9. M. H. Meteab, A. Hashim, and B. H. Rabee, *Opt. Quant. Electron.*, **55**: 187 (2023); <https://doi.org/10.1007/s11082-022-04447-4>
10. H. Ahmed and A. Hashim, *Silicon*, **14**: 7025 (2021); <https://doi.org/10.1007/s12633-021-01465-x>
11. M. H. Meteab, A. Hashim, and B. H. Rabee, *Silicon*, **15**: 251 (2023); <https://doi.org/10.1007/s12633-022-02020-y>
12. M. H. Kadhim, A. S. Hasan, M. A. Akraa, and A. Y. Layla, *Journal of Ovonic Research*, **17**: 3 (2021); doi.org/10.15251/jor.2021.173.273
13. Y. Son, M. Cohen, and S. Louie, *Nature*, **444**: 7117 (2006); <https://doi.org/10.1038/nature05180>
14. A. S. Hasan and H. I. Abbood, *Journal of Kufa-Physics*, **8**: 59 (2016); <https://journal.uokufa.edu.iq/index.php/jkp/article/view/7474>
15. S. Hu, L. Collins, V. Goncharov, J. Kress, R. McCrory, and S. Skupsky, *Physics of Plasmas*, **23**: 4 (2016); <https://doi.org/10.1063/1.4945753>
16. F. Q. Mohammed, M. S. Edan, A. S. Hasan, and A. J. Haider, *Key Engineering Materials*, **886**, No. 1: 97 (2021); doi.org/10.4028/www.scientific.net/KEM.886.97
17. Z. Huang, M. Shanmugam, Z. Liu, A. Brookfield, E. Bennett, R. Guan, D. Vega Herrera, J. Lopez-Sanchez, A. Slater, E. McInnes, X. Qi, and J. Xiao, *Journal of the American Chemical Society*, **144**: 14 (2022); <https://doi.org/10.1021/jacs.2c01410>
18. A. S. Hasan, B. Y. Kadem, M. A. Akraa, and A. K. Hassan, *Digest Journal of Nanomaterials and Biostructures*, **15**: 1 (2020); doi.org/10.15251/djnb.2020.151.197
19. A. S. Hasan, F. Q. Mohammed, and M. M. Takz, *Journal of Mechanical Engineering Research and Developments*, **43**: 11 (2020); [https://jmerd.net/Paper/Vol.43,No.1\(2020\)/11-17](https://jmerd.net/Paper/Vol.43,No.1(2020)/11-17)
20. X. Zhang, Z. Chen, Z. Wan, C. Liu, R. He, X. Xie, and Z. Huang, *International Journal of Molecular Sciences*, **23**: 20 (2022); <https://doi.org/10.3390/ijms232012158>
21. S. A. Habeeb, A. S. Hasan, T. Ąlu, and A. J. Jawad, *Iranian Journal of Chemistry and Chemical Engineering*, **40**: 5 (2021); doi.org/10.30492/ijcce.2020.40535
22. T. Chantawansri, T. Sirk, E. Byrd, J. Andzelm, and B. Rice, *Journal of Chemical Physics*, **137**: 20 (2012); <https://doi.org/10.1063/1.4767394>
23. S. H. Abud, A. S. Hasan, M. Almaamori, and N. Bayan, *Journal of Physics*:

- Conference Series*, **1818**: 1 (2021); doi.org/10.1088/1742-6596/1818/1/012235
24. K. Johnston and V. Harmandaris, *Soft Matter*, **8**: 23 (2012); <https://doi.org/10.1039/c2sm25567g>
 25. A. D. T. Thamira, A. S. H. Hasan, R. G. K. Kadhim, W. G. B. Bakheet, and H. I. Abbood, *Journal of Petroleum Research and Studies*, **8**: 3 (2021); doi.org/10.52716/jprs.v8i3.228
 26. Y. Kong, M. Tao, X. Cao, Z. Wang, and B. Xing, *Journal of Hazardous Materials*, **459**: 1 (2023); <https://doi.org/10.1016/j.jhazmat.2023.132071>
 27. B. Y. Kadem, M. Al-Hashimi, A. S. Hasan, R. G. Kadhim, Y. Rahaq, and A. K. Hassan, *Journal of Materials Science: Materials in Electronics*, **29**: 1 (2018); doi.org/10.1007/s10854-018-0055-4
 28. S. K. Jebur, A. J. Braihi, and A. S. Hassan, *Materials Today: Proceedings*, **49**: 7 (2022); doi.org/10.1016/j.matpr.2021.09.255
 29. R. Akbarzadeh, O. Ayeler, Q. Ibrahim, P. Olubambi, and P. Ndungu, *Heliyon*, **8**: 2 (2022); <https://doi.org/10.1016/j.heliyon.2022.e08903>
 30. A. A. Ati, A. H. Abdalsalam, and A. S. Hasan, *Journal of Materials Science: Materials in Electronics*, **32**: 3 (2021); doi.org/10.1007/s10854-020-05053-4
 31. J. Soler, F. Artacho, J. Gale, A. García, J. Junquera, P. Ordejón, and D. Sánchez-Portal, *Journal of Physics: Condensed Matter*, **14**: 11 (2002); <https://doi.org/10.1088/0953-8984/14/11/302>